INTERNATIONAL JOURNAL OF ENVIRONMENT
Volume-13, Issue-1, 2024 ISSN 2091-2854
Received: 9 May 2024 *Revised: 25 September 2024* *Accepted: 2 October 2024*

ADSORPTION OF LEAD, ARSENIC AND MERCURY FROM INDUSTRIAL EFFLUENT USING LOW-COST AGRO-WASTE

B. Tijjani [1]*, A.L. Yaumi [2], H.D. Mohammed [2], H. Umar [2], E. Yakubu[1], B. K. Highina[2]
[1]Department of Chemical Engineering, School of Engineering and Engineering Technology, Federal University of Technology, Owerri, Nigeria
[2]Department of Chemical Engineering, Faculty of Engineering, University of Maiduguri, Nigeria
*Corresponding author: brahtijjani@gmail.com

Abstract

Heavy metal contamination in industrial effluents poses significant environmental and health risks, necessitating the development of effective, low-cost adsorbents. This study explored the potential of Millet Husk and Millet Straw, agricultural waste materials, for the removal of Lead (Pb), Arsenic (As), and Mercury (Hg) from industrial effluents. Millet Husk and Millet Straw activated carbon (MHS) was prepared through sodium hydroxide (NaOH) activation and characterized using Scanning Electron Microscopy (SEM), Fourier Transform Infrared Spectroscopy (FT-IR), X-Ray Diffraction (XRD), and Energy Dispersive X-ray Spectroscopy (EDX). Batch adsorption experiments were conducted to assess the performance of MHS in removing heavy metals from effluent samples, with removal efficiency analyzed using Atomic Absorption Spectrometry (AAS). Characterization results revealed that MHS exhibited enhanced surface morphology, high porosity, and functional groups that facilitated heavy metal adsorption. The optimal removal efficiencies were 58.67% for Pb, 69.83% for As, and 100% for Hg. Factors such as adsorbent dosage, contact time, and pH significantly influenced adsorption rates, with maximum adsorption observed at a dosage of 0.1 g. The study concluded that MHS is a promising adsorbent for heavy metal removal from wastewater, with its adsorption capacity dependent on initial metal concentrations and pH levels. Further research is recommended to explore the scalability of MHS in real-world applications, investigate modifications to enhance its adsorption capabilities, and study its regeneration and reuse potential for long-term viability as an eco-friendly adsorbent.

Keywords: Activated carbon, Adsorption, Arsenic, Lead, Mercury

DOI: https://doi.org/10.3126/ije.v13i1.70629

1. Introduction

In the past few decades, urbanisation, industry, and agricultural practises have all contributed to a large increase in the outflow of wastewater that is contaminated with metal ions. Wastewater is often separated into two categories: home wastewater and industrial wastewater. Wastewater originating from household sources might include hazardous compounds, bacteria, viruses, sewage, non-toxic organisms, detergents, and trash. It is composed of both liquid and solid wastes produced by non-manufacturing operations. However, untreated wastewater released by industries is the main cause of water contamination. Among the toxins present in industrial wastewater that find their way into the environment are dyes, aromatics, pesticides, heavy metals, oil, and other hazardous substances that pose a major risk to both human health and the ecosystem (Nallakukkala et al., 2022). Because of the accelerated rate of urbanisation and growth, as well as the discharge of industrial and municipal effluents that threaten the survival of aquatic life, rivers are under excessive stress (Khan et al., 2021). A wide range of living things may suffer when exposed to heavy metals in the environment. The primary characteristic that sets heavy metals apart from other harmful contaminants is their inability to biodegrade and even their propensity to accumulate in living things. For this reason, removing heavy metals from wastewater is crucial for maintaining public health (Biiyiikgiingor, 2018).

Excessive concentrations of metals like Cd, Pb, Hg, and As are very bad for the environment (Ignatowicz, 2017). Due to heavy metals' extensive use in technical, industrial, and agricultural applications, they are now major environmental contaminants that pose a threat to human health worldwide. Heavy metals that are biologically necessary, such as iron, manganese, and zinc, are vital nutrients needed for a variety of physiological processes. Other elements that are classified as non-essential metals include arsenic, cadmium, lead, and mercury. Even at low levels of exposure, the majority of these heavy metals can cause harm to various organs or systems. Cadmium, lead, mercury, and arsenic are among the most dangerous metals and are ranked in the top 10 on the Agency for dangerous Substances and Disease Registry's Substance Priority List (Wang & Matsushita, 2021).

A variety of techniques have recently been studied in an effort to improve treated water quality while simultaneously reducing the amount of wastewater produced in a cost-effective and efficient manner (Nallakukkala et al., 2022). The most suitable method for removing heavy ions from wastewater will depend on a number of important factors, such as the cost of operation, the metal

ions' initial concentration, the environmental impact, pH levels, chemicals added, removal efficiency, and economic viability. Chemical treatments (chemical precipitation, coagulation-flocculation, flotation, reduction, electrocoagulation (EC), electro-flotation (EF), and advanced oxidation), electric treatments (i.e., electrochemical (reduction, EC, EF, and advanced oxidation) and ion exchange), membrane treatments (ultrafiltration (UF), nanofiltration, microfiltration, reverse osmosis, forward osmosis, and electro-dialysis), and photocatalysis are the categories into which these techniques fall (Qasem & Mohammed, 2021). Adsorption has several advantages over traditional treatment methods, such as a straightforward design, cheap cost, high effectiveness, no chemical or biological sludge, no need for extra nutrients, adsorbent regeneration, and the potential for metal recovery (Batagarawa et al., 2017).

Wastes from agriculture frequently cause environmental issues (Abba et al., 2017). Since of their loose structure and porous nature, agricultural wastes are extremely sensitive adsorbents since they include a variety of reactive functional groups, such as hydroxyl and carboxyl groups (Al-ghouti & Da, 2020). The Food and Agriculture Organisation (FAO) reported that between 2003 and 2013, millet production covered between 29 and 38 million hectares. In 2013, the world produced 29.8 million tonnes of millet, of which 5 million tonnes were produced in Nigeria, with the country's north producing more than 80% of the grain. Nigeria, which now produces second-most pearl millet worldwide, accounting for 16.7% of production worldwide, rose from third place to the top in the world rankings. In the states of Borno and Adamawa, respectively, pearl millet production occupies more than 60% of croplands. (Adegbola & Otitodun, 2023). In Nigeria, an estimated 2.76 million tonnes of millet plant residue are produced annually (Ajikashile et al., 2023). The present research focused on the potentials of using millet husk and millet straw as adsorbents for the adsorption of Lead, Arsenic, Mercury from industrial effluent.

2. Materials and methods

2.1 Sample collection

The materials utilized in this work were millet husk and millet straw, both materials were collected in a polyethene bags from farm site (with coordinates: 11.801740, 12.488765) in Benisheikh, Kaga Local Government Area, Borno State, Nigeria. The millet husk was handpicked to remove dirty particles and washed with tap water several times to get rid of adhering particles. The millet straws were cut into pieces and were similarly washed with clean water repeatedly to remove moisture

soluble impurities. Both samples were rewashed thoroughly with distilled water, and later drained, sun-dried for 12 hours. The dried samples were stored in air-tight containers for further analyses. The sample effluent was collected in a 5 litres polyethene can from the Coca-Cola Bottling Company, Maiduguri, Borno State, Nigeria. The sample were labelled appropriately and brought to the laboratory for further analysis.

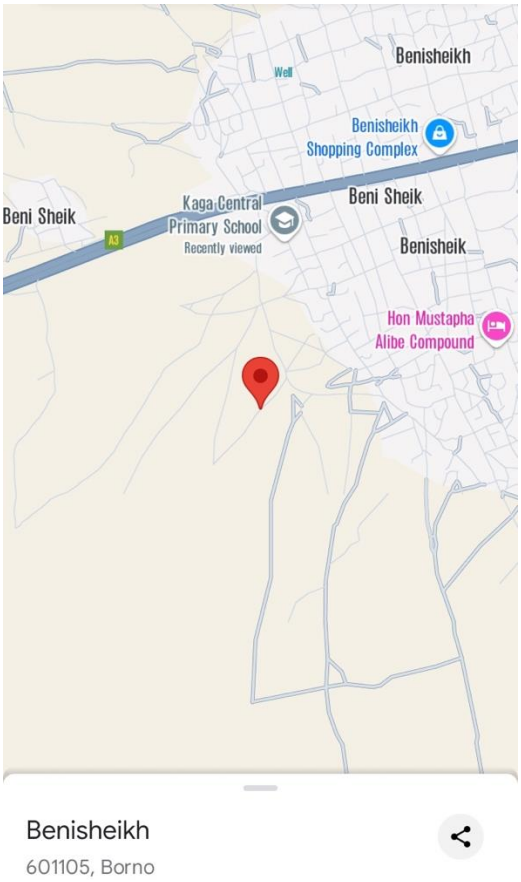

Figure 2.1. Location Map of farm site

2.2 Carbonization and Chemical Activation

The dried samples were carbonized at 500°C for 2hrs in muffle furnaces. The carbonized samples were milled using mortar and pestle to get a powder form. The carbonized samples were sieved with a 300 µm mesh, weighed, and each sample was divided into three equal parts. The divided samples were activated with 1 molarity (1M), 2 molarity (2M), and 3 molarity (3M) of NaOH solutions for 48hr at room temperature. After impregnation, samples were then filtered, oven-dried at 105°C for 90min so as to remove moisture completely. The activated carbons produced were washed with 0.5 M HCl acid solution, filtered and washed several times with distilled water to obtain fairly constant pH. The samples were oven-dried at 250°C, and labelled MH_1, MH_2, and

MH_3 for millet husk; and MS_1, MS_2 and MS_3 for millet straw respectively. The subscripts 1, 2, and 3 represent the impregnation molarities of the prepared activated-carbons.

2.3 Characterization of Adsorbent

The activated-carbon was characterized using Fourier transform infrared spectroscopy (FT-IR), Scanning electron microscopy (SEM), X–ray spectrometry (EDX) and X-ray diffraction spectra (XRD) to study their functional groups, the morphologies, elemental chemical composition and crystallographic phase structures of the activated-carbon (MHS).

2.3.1 Fourier Transform Infrared Spectroscopy (FT-IR)

Fourier Transform Infrared Spectroscopy (FT-IR) was used to characterize the main functional groups of the activated-carbon surface using a FTIR spectrometer (Jasco FTIR 4100 series spectrophotometer with a diffuse reflectance accessory manufactured by PIKE Technologies); samples of activated-carbon were mixed with finely divided spectroscopic-grade KBr with a resolution of 4 cm^{-1} varies up to 0.125 cm^{-1} in range of 4000 cm^{-1} to 400 cm^{-1}.

2.3.2 X-ray Diffraction spectra (XRD)

X-ray Diffraction spectra (X-ray Diffractometer Thermo scientific model: ARL'XTRA X-ray and serial number197492086) is a powerful characterization that describes crystalline information as structures, phases, texture, strains, crystal defects, and lattices. XRD diffraction peaks are produced through monochromatic beam of X-rays scattering through the lattice plane by diffraction angles (θ). X-ray intensity is obtained from the atomic position present in each lattice plane. Powder X-ray diffraction (XRD) experiments were performed between 2° and 70° (2θ) with a step size of 0.02° and a measuring time of 0.8 s per step using a Bruker D8 Advance diffractometer with Cu-Kα (λ = 0.154 nm) radiation operating at 40 kV and 40MA and identified using JCPDS file.

2.3.3 Scanning Electron Microscopy (SEM) and Energy Dispersive X–ray (EDX)

The Scanning Electron Microscopy (SEM model Phenom ProX, by PhenomWorld Einhoven, Netherlands) and Energy Dispersive X–ray spectrometry (SEM model: Pro:X: 800-07334 Phenom World and Serial Number MVE01570775) experiments were carried out on the composite adsorbent (MHS) at accelerating voltage of 10KV, beam size 3.0 and of different magnifications. The micrographs before and after the adsorption of metal ions were taken and compared to study

the morphology and to determine the elemental analysis before and after adsorption of the activated carbons, which allowed us to determine the elemental mapping of the samples.

2.4 Batch Adsorption Experiments

A 0.5 g each of the MH_1, MH_2, and MH_3 were soaked in 50 mL of the effluent water in 500 mL beakers at a constant shaking speed of 250 rpm for 60 min using flocculation apparatus (edibon Spain). Similar procedure was followed to carried out for the Millet straw. All the experiments were carried out at room temperature 25°C. The mixtures were finally filtered using Whatman Cat No 1001 110 filter papers, then the filtrates and the raw effluent samples were analyzed for initial and residual metal ions concentration by an Atomic Absorption Spectrophotometer (AAS). A composite activated-carbon (MH_1, MH_2, MS_1 and MS_3) was produced based on their performance from the first experiments. The heavy metals (As, Pb and Hg) present in samples were determined by using Atomic Absorption Spectro-photometric (AAS) method.

2.4.1 Effect of Dosage

The effect of adsorbent dosage on the removal of heavy metals was investigated by varying the dosage from 0.1 g to 0.7 g while keeping the other parameters constant (contact time: 30 minutes, agitation rate: 250 rpm, temperature: 25 °C, initial concentrations of Pb, As, and Hg: 0.721, 0.358, and 0.026 mg/L respectively, and pH: 6.06).

The percentage removal and amount of adsorption at equilibrium were obtained using equations (1) and (2).

$$\%\, Removal = \frac{(C_0 - C_e)}{C_0}\ X\ 100 \qquad 1$$

$$q_e = \frac{(C_0 - C_e)V}{W} \qquad 2$$

Where C_o and C_e are the concentrations (mg/L) of metal Ions initially and at equilibrium time W is the weight of the adsorbed (mg), q_e is the amount of metal ion adsorbed (mg/g), while V is the volume of the solution in litre.

2.4.2 Effect of Contact Time

To determine the optimum contact time for maximum adsorption, a series of experiments were conducted by varying the time from 20 to 120 minutes while keeping other parameters constant (dosage: 0.1 g, agitation rate: 250 rpm, temperature: 25 °C, initial concentrations of Pb, As, and

Hg: 0.721, 0.358, and 0.026 mg/L respectively, and pH: 6.06). The removal efficiencies were calculated, and samples were analyzed for heavy metal content at each time interval.

2.4.3 Effect of pH

The influence of pH on adsorption efficiency was studied by adjusting the pH of the effluent solution (4.25, 6.06, 7.42, and 9.94) either with 1M H_2SO_4 or 1M NaOH using pH meter to equilibrate the desired value, while keeping other parameters constant (dosage: 0.1 g, agitation rate: 250 rpm, contact time: 30 minutes, temperature: 25 °C, initial concentrations of Pb, As, and Hg: 0.721, 0.358, and 0.026 mg/L respectively.

2.4.4 Effect of Initial Concentration

To examine the effect of initial metal ion concentration on adsorption, experiments were conducted by varying the concentrations from 20 to 140 mg/L while maintaining constant conditions (dosage: 0.1 g, agitation rate: 250 rpm, contact time: 30 minutes, and pH: 7).

3. Results and discussion

3.1 Characterization of Adsorbents

3.1.1 Fourier Transform Infrared Spectroscopy

The FTIR spectra can provide valuable information about the chemical compositions of the materials. Figure 3.1(a), (b), (c) and (d) showed the FTIR absorption spectra of RMH, RMS, MHS-B and MHS-A to confirm the presence of different functional groups (such as hydroxyl, alkanes, esters, aromatics, etc.) in the adsorbent.

The FTIR adsorption spectra of RMH (Figure 3.1a) shows a broadband at 3317.3 cm^{-1} which indicates the presence of hydrogen-bonded -OH stretching from alcohol and phenols and is also dominated by -NH stretching. The bands at 2922.2 cm^{-1} and 2855.1 cm^{-1} in IR spectra of RMH may be due to the C–H (alkanes) stretching vibrations (Hashem et al., 2016). Peaks at 1632.6 and 1513.3, 1423.8 and 1371.7, 1237.5 and 1162.9, 1028.7, and 834.9 cm^{-1} corresponded to the C=O (esters), C–C (aromatics), C–H (alkanes), C–O (alcohols, carboxylic acids, esters, ethers), C–X (alkyl halide) (Abbas & Ahmed, 2016).

The FTIR absorption spectra of RMS (Figure 3.1b) shows a broadband at 3339.7 cm^{-1} which indicates the presence of hydrogen-bonded -OH stretching vibration and is also dominated by -NH stretching vibration. Also, the bands at 2922.2 cm^{-1} in IR spectra of RMS may be owing to the C–H (alkanes) stretching vibrations (Hashem et al., 2016). Peaks at 1736.9 and 1602.8, 1416.4 and 1319.5, 1237.5, and 1028.7 cm^{-1} corresponded to C=O (esters), C–C (aromatics), C–H (alkanes), C–O (alcohols, carboxylic acids, esters, ethers) (Abbas & Ahmed, 2016). It can be observed that the precursor RMH has much more contents of aliphatic C-H group and also it has comparatively high numbers of peak with that of the RMS (Byamba-ochir et al., 2016).

Figure 3.1(c) and (d) depicted the FTIR spectra of MHS-B before and MHS-A after adsorption, it is noteworthy that there are shifts and complete disappearances of the characteristic peaks after the adsorption process. The absorption bands at 3026.6, and 2922.2 cm^{-1} indicate the stretching vibration of hydroxyl and alkane, groups respectively (Seh-bardan, 2013), whereas the bands at 879.7 and 752.9 cm^{-1} are as result of out-of-plane deformation mode of C–H for different substituted benzene rings (Yakout & El-deen, 2016). The spectra of these groups shifted to 3041.5, 2907.3, 872.2 and 745.5 cm^{-1} after adsorption of As, Hg and Pb, respectively. The shift in the hydroxyl and alkane groups spectra indicate their involvement in the adsorption process (Yakout & El-deen, 2016). The disappearance of the peaks after adsorption may be attributed to formation of chemical bonds, monolayer, surface restructuring, blockage of active sites, change in molecular symmetry or electronic effects.

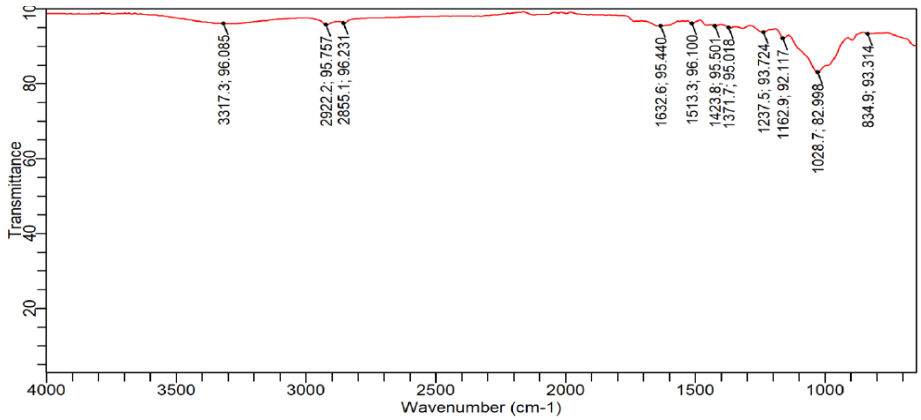

Figure 3.1(a): FT-IR spectra of RMH

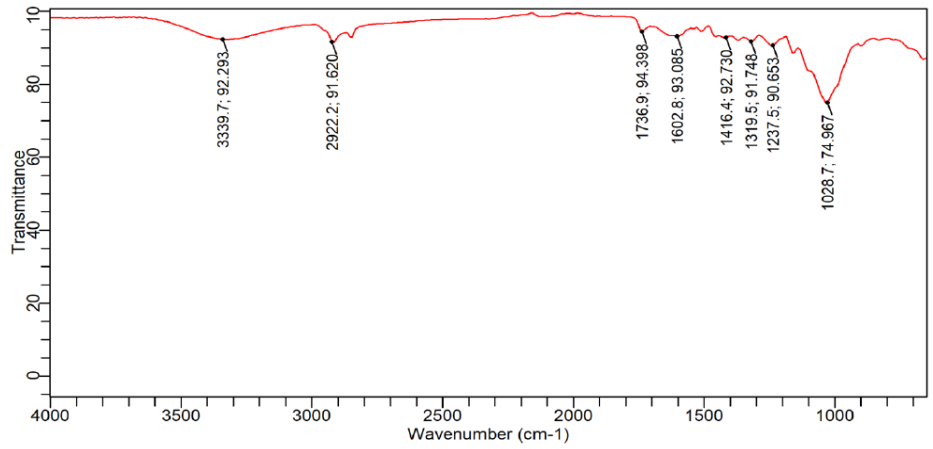

Figure 3.1(b): FT-IR spectra of RMS

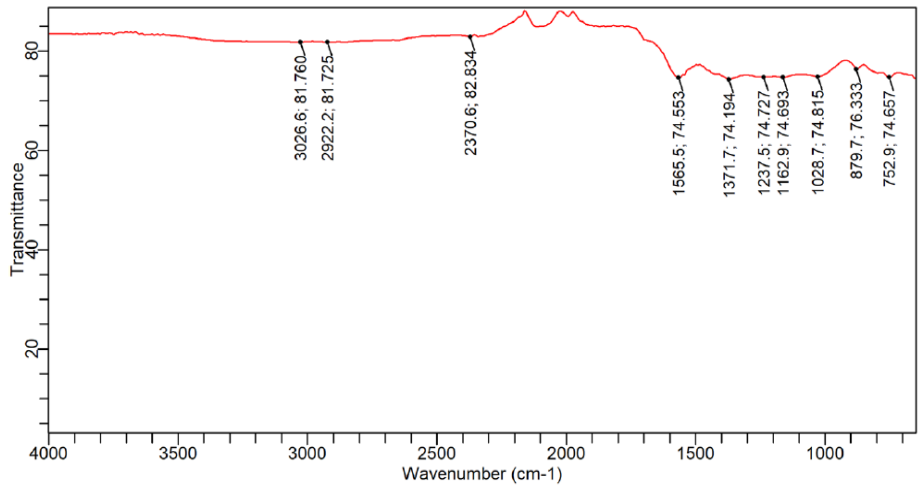

Figure 3.1(c): FT-IR spectra of MHS adsorbent before adsorption

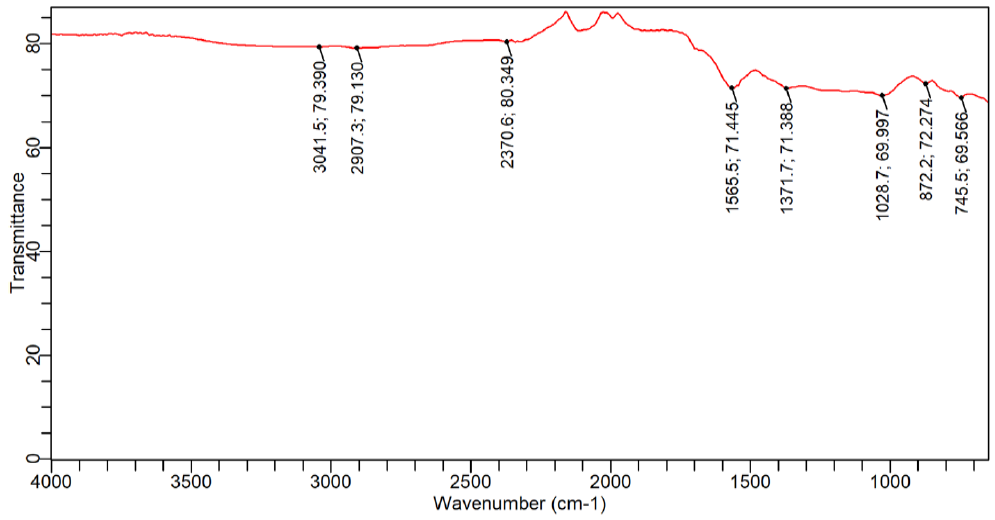

Figure 3.1(d): FT-IR spectra of MHS adsorbent after adsorption

3.1.2 X-ray diffraction (XRD) analysis

X-ray diffraction (XRD) analysis was performed to understand the influence of lignocellulosic composition on the hard carbon formation as a function of the degree of crystallinity. The X-ray diffractograms of RMH, RMS, and MHS before and after adsorption are presented in Fig. 3.2 a-d. The patterns for RMH and RMS showed largely amorphous area and one characteristic peak around 21.77° at d=4.078Å and 21.93° at d=4.049Å respectively, which represent cellulose structure I, commonly observed in plants(Yadav et al., 2019).

The pattern for MHS before adsorption showed a combination of sharp and broad peaks, and amorphous hump was 39.68° at d=2.270Å. The sharp peaks were 34.15° at d=2.6237Å, 37.968° at d=2.3679Å, 44.19° at d=2.0481Å, and the broad was 64.43° at d=1.4449Å. The hump at 2θ=39.68° is associated with the disordered regions or amorphous phase(Arslan et al., 2022) while the peak at 2θ=44.19° corresponds to crystalline peak associated with cellulosic carbon of MHS(Prajapati et al., 2022). Delignification as a result of the alkali treatment might be causes of the dissolution of amorphous components(Yadav et al., 2019). After adsorption the peaks and hump were slightly increased in intensity and marginally shifted to 34.176° at d=2.6215Å, 37.999° at d=2.3661Å, 39.74° at d=2.267Å, 44.203° at d=2.0473Å, 64.413° at d=1.4453Å. This might be due to surface adsorption of Pb, As, and Hg onto the MHS(Prajapati et al., 2022). Furthermore, a new peak was observed around 68.80° at d=1.3635Å, signifying several phenomena, including the

formation of new crystalline phases resulting from the interaction between the absorbate and the adsorbent surface(Joga Rao, 2021), structural changes that alter the crystal structure of the adsorbent leading to shifts in existing peaks or the emergence of new ones due to changes in crystallinity (Elavarasan, 2018), and chemical reactions between the adsorbate and the functional groups on the adsorbent, reflecting changes in bonding and molecular structure (Siswati et al, 2023).

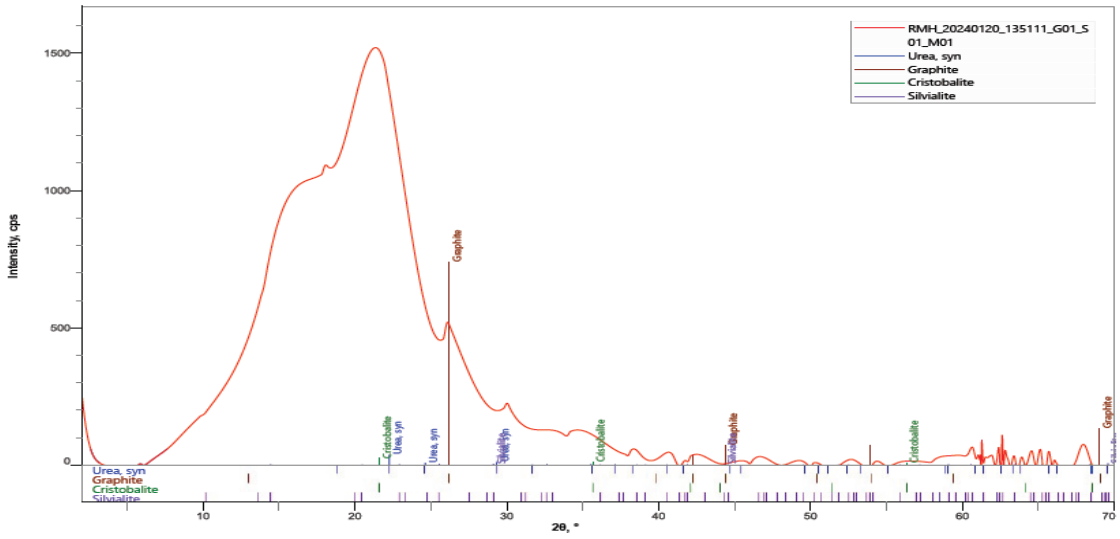

Figure 3.2a: XRD pattern of RMH

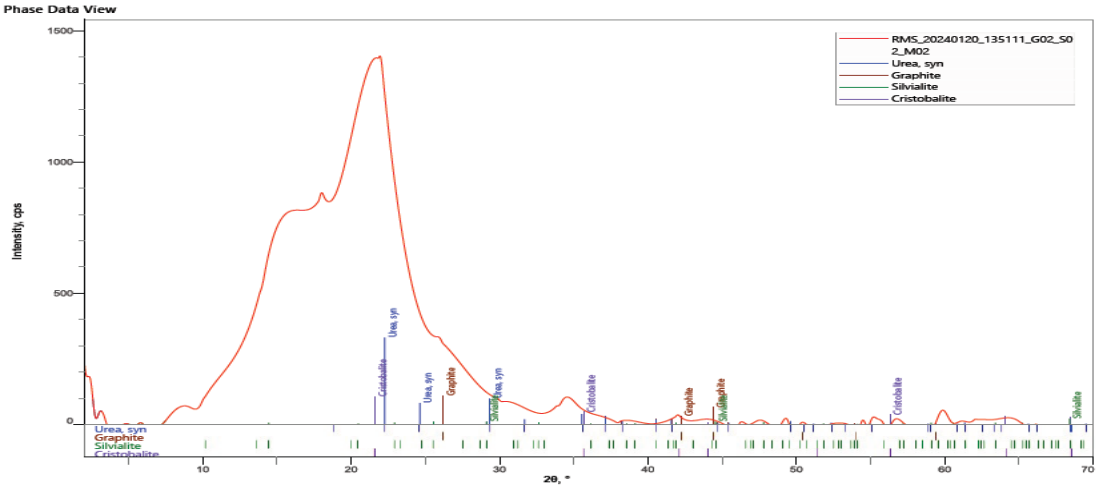

Figure 3.2b: XRD pattern of RMS

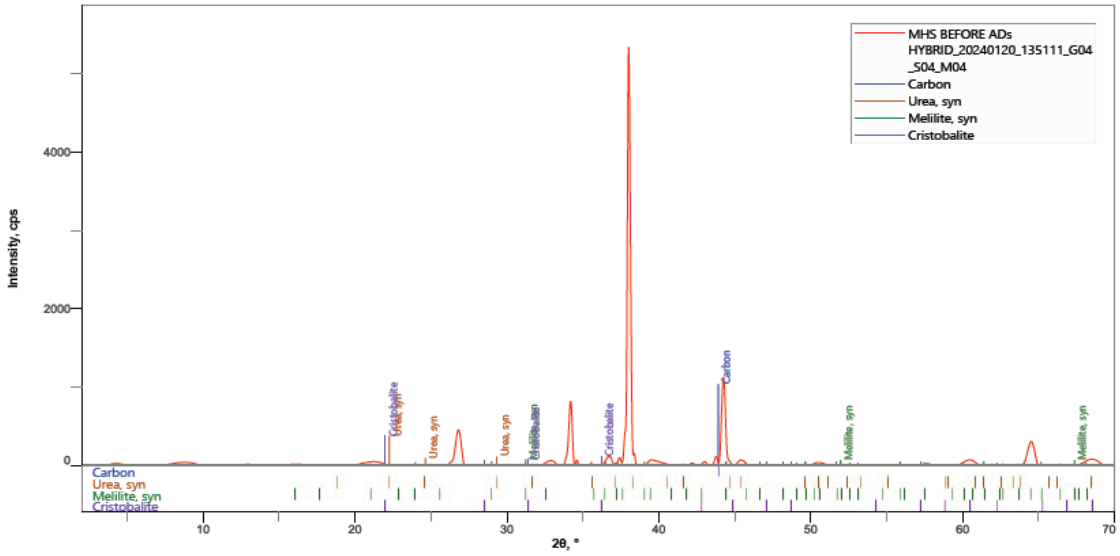

Figure 3.2c: XRD pattern of MHS Before

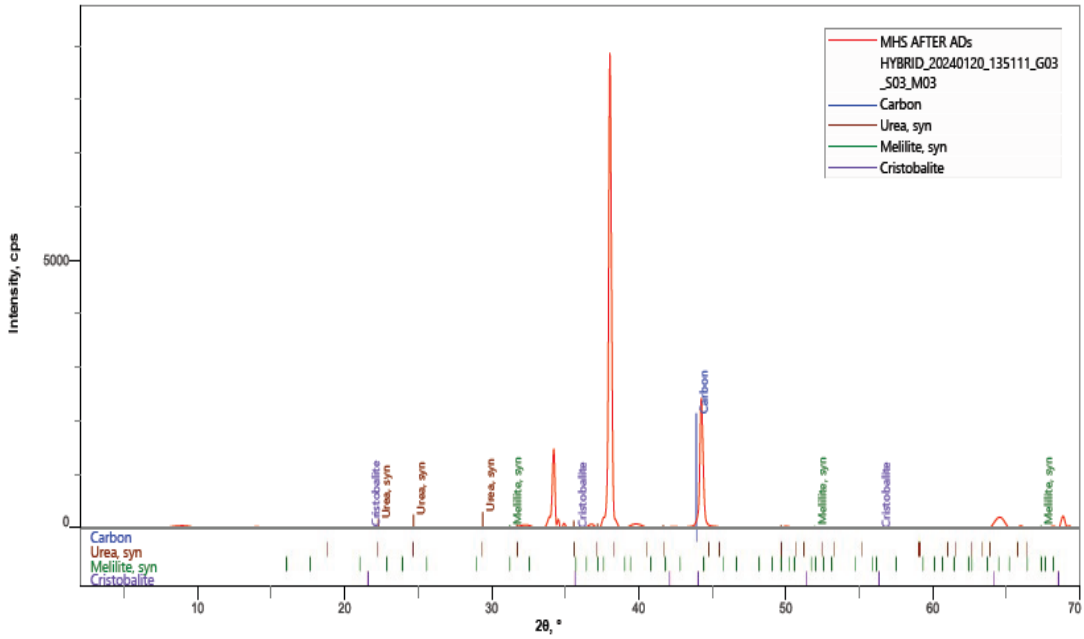

Figure 3.2d: XRD pattern of MHS After

3.1.3 Scanning Electron Microscopy (SEM)

Scanning Election Microscopy (SEM) has been extensively used to characterize the microstructure of raw millet husk (RMH), raw millet straw (RMS), hybrid of millet husk and millet straw activated carbons before and after adsorption which revealed the porous nature of the adsorbents and an

increase in surface porosity, such that physical adsorption played a major role in the overall sorption process (Tatah, et al., 2017). SEM images were taken to compare the native morphological differences between the precursors, RMH and RMS, and that of the hybrid adsorbent, MHS before and after adsorption. Figure 3.3 (a and b) shows the SEM images of RMH and RMS respectively, and it clearly indicated that the surfaces of the two precursors are distinguishable. The SEM in Figure 3.3(c) showed partially developed honey comb-like and highly defined pores. It shows that, carbonization influenced the topographical characteristics of the adsorbents. Figure 3.3(d) shows the surface structure after adsorption of Pb, As and Hg metals from the effluent. The image revealed that the external surface contains of small cavities, characterized by irregular heterogeneous surface which suggested presence of adsorbed metal ions on the surface. Before carbonization and activation for both precursors, the images revealed that the external surface was full of cavities, roughly characterized by irregular heterogeneous surface which suggested that, the raw millet husk and millet straw exhibit high surface area, however, the hybrid adsorbent before adsorption has more distinguish pores than that of its raw precursors, indicating that it will have more surface area than the precursors, and large surface area increased the rate of adsorption. Disappearance of some pores and lighter surface of the adsorbent after metal ion adsorption suggested that, metal ions adsorption had taken place (Figure 4.3d).

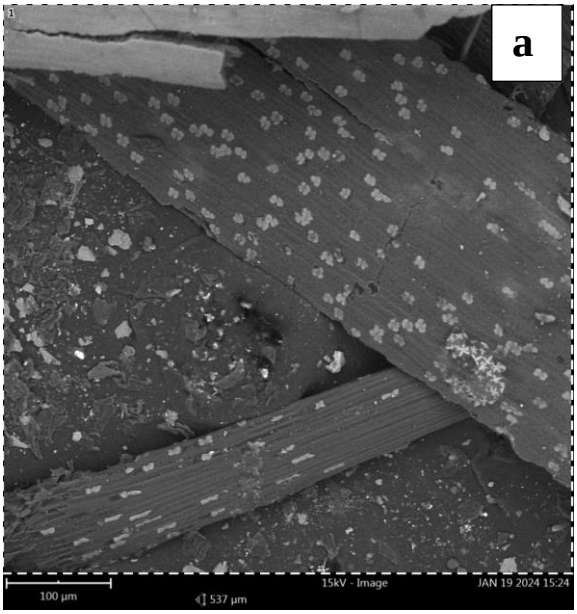

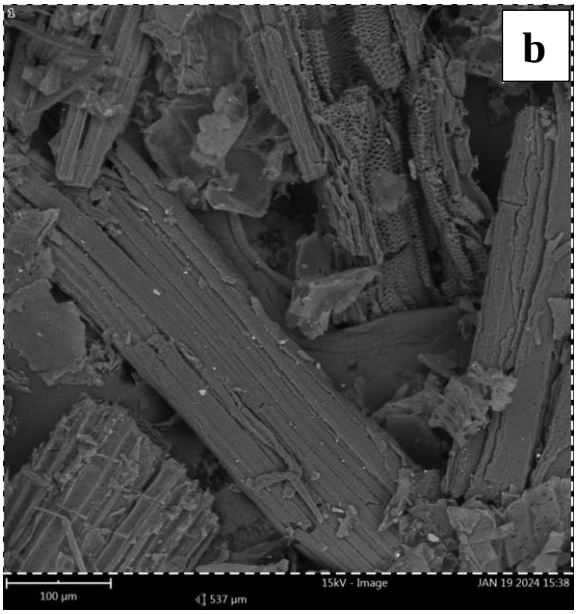

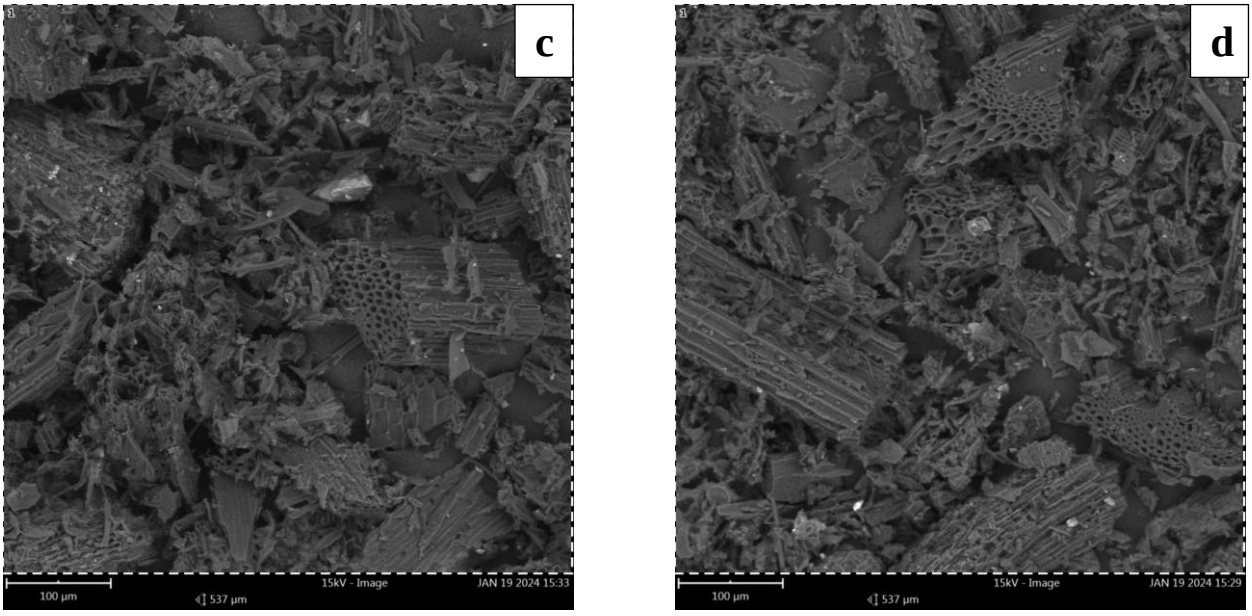

Figure 3.3: SEM analysis of RMH (a), RMS (b), MHS Before adsorption (c), and MHS After adsorption (d)

3.1.4 Energy-dispersive X-ray spectroscopy (EDX) Analysis

Energy-dispersive X-ray spectroscopy (EDX) measurements were performed for precursors and adsorbent (before and after adsorption) as presented in Table 3.1 and figure 3.4 (a-d). Elemental analysis indicates higher carbon wt.% content in the RMH than RMS, while the MHS-A has higher content than MHS-B, suggesting that the adsorbate contains a significant amount of carbon, which can occur due to adsorption of organic compounds adding carbon to the adsorbent, chemical interaction where carbon-containing functional groups from the adsorbate bond to the surface of the adsorbent, and surface modifications that enhance the ability of the adsorbent to retain carbon-rich species (Bedmohata et al, 2015). Additionally, elements other than carbon; for example, the RMH and MHS-B have N, Na, Mg, Al, Si, P, S, Cl, K, Ca and Fe, while the RMS has all the aforesaid elements except Fe, and the EDX spectra after adsorption of Pb, As and Hg have revealed the existence of all the aforementioned elements on MHS-A with addition of Ti.

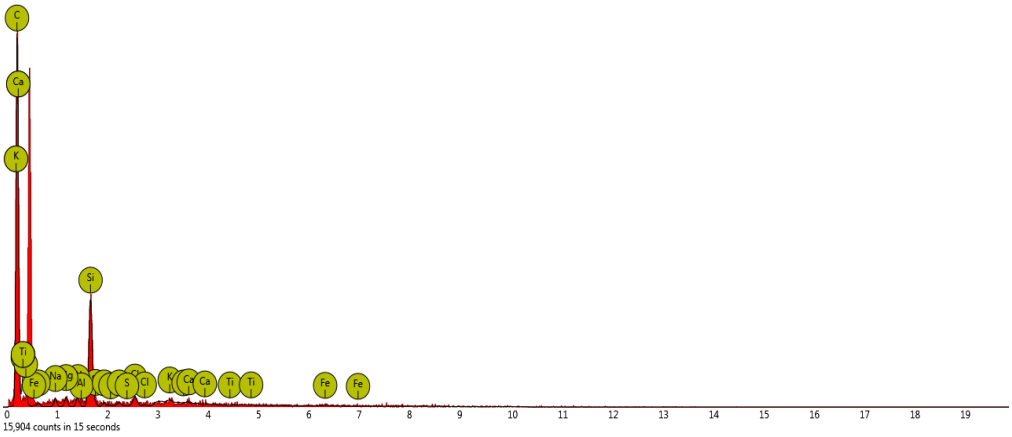

Figure 3.4a EDX Analysis of RMH

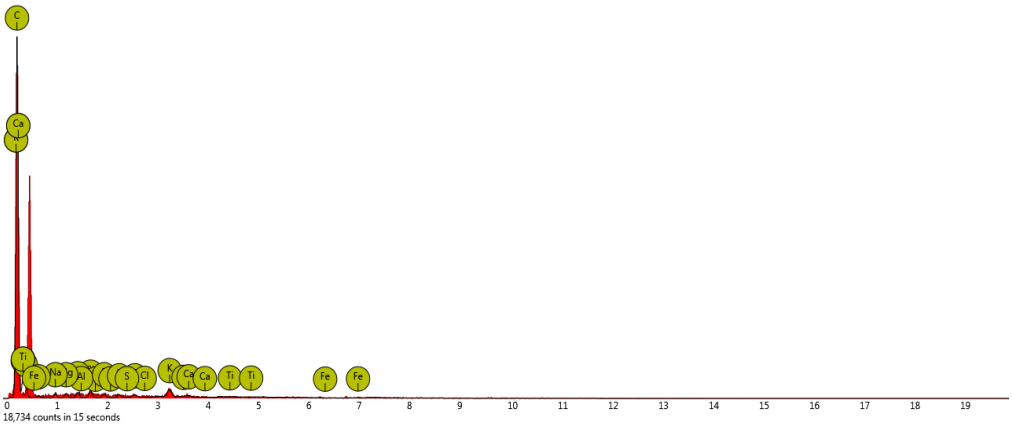

Figure 3.4b: EDX Analysis of RMS

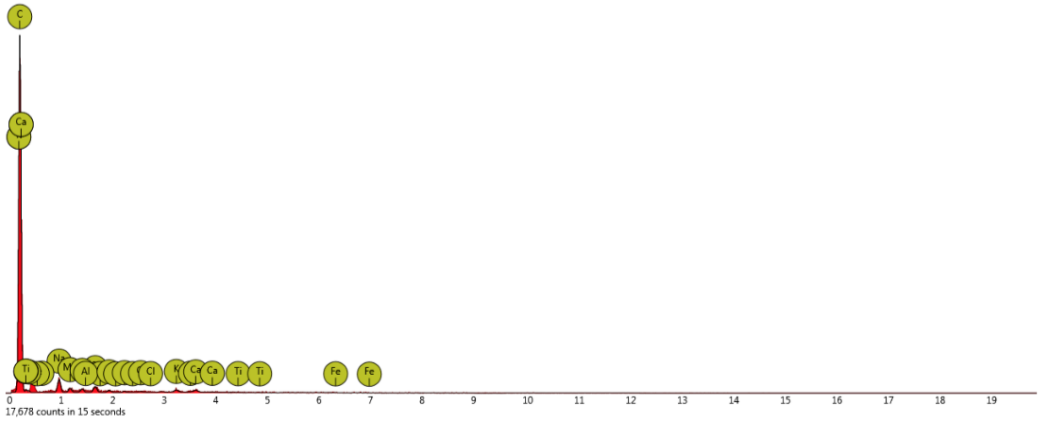

Figure 3.4c: EDX Analysis of MHS Before Adsorption

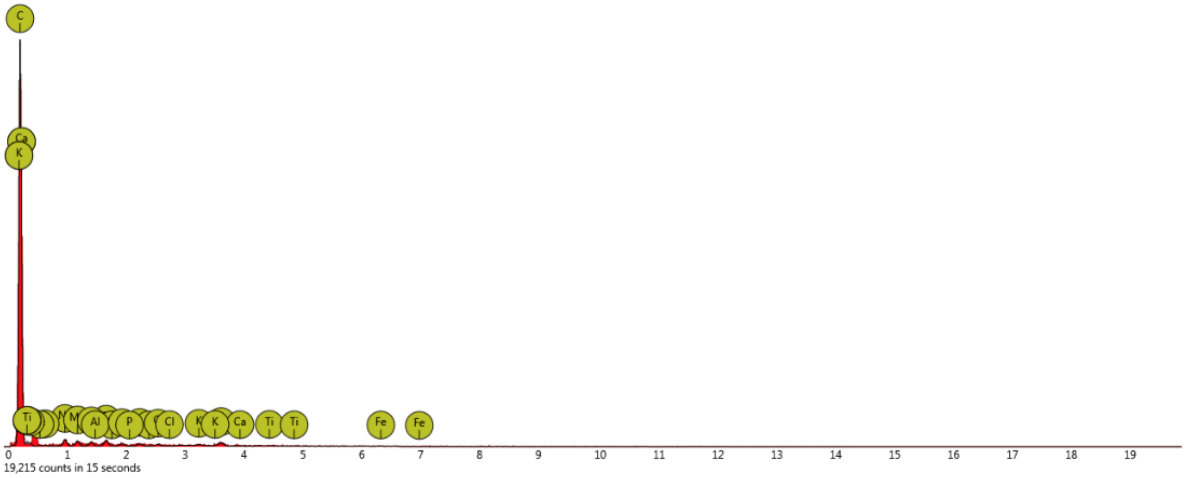

Figure 3.4d: EDX Analysis of MHS After Adsorption

The EDX analysis (Fig.3.4) shows that the exchangeable cations and anions of N^{3-} Na^{+}, Si^{4+}, K^{+} and Fe^{3-} concentrations in MHS decrease from 7.95, 11.87, 3.06, 2.15, and 0.60 wt/wt to 7.92, 6.01, 2.78, 1.15 and 0.51 respectively after adsorption. These results suggest that a cation exchange had taken place between exchangeable cations and the heavy metals adsorbed, thereby significantly enhancing adsorption capacity onto MHS. In addition to the cation exchange process, negatively charged surface, water absorption process and surface morphology could also contribute to adsorption process. The above mentioned aspects may have synergistically contributed to the high adsorption capacity and removal efficiency for Pb, As and Hg on MHS (Alshameri et al., 2017).

Table 3.1 Elemental analysis of RMH, RMS, MHS before and after adsorption

Precursor/Adsorbent			RMH		RMS		MHS-B		MHS-A	
Element	Element	Element	Atomic	Weight	Atomic	Weight	Atomic	Weight	Atomic	Weight
Number	Symbol	Name	CONC	CONC	CONC	CONC	CONC	CONC	Concentration	Concentration
6	C	Carbon	67.36	51.83	72.34	59.09	76.83	64.09	79.75	67.46
7	N	Nitrogen	12.46	11.18	14.45	13.77	8.18	7.95	8.03	7.92
11	Na	Sodium	2.16	3.19	2.47	3.86	7.43	11.87	3.71	6.01
12	Mg	Magnesium	1.62	2.52	1.62	2.69	1.88	3.18	2.02	3.45
13	Al	Aluminium	1.24	2.14	1.52	2.79	1.14	2.15	1.2	2.29
14	Si	Silicon	11.72	21.08	1.56	2.97	1.57	3.06	1.41	2.78
15	P	Phosphorus	0.61	1.22	1.21	2.54	0.62	1.33	0.69	1.5
16	S	Sulfur	0.48	0.98	0.76	1.66	0.31	0.68	0.69	1.55
17	Cl	Chlorine	1.52	3.45	0.87	2.11	0.3	0.74	0.61	1.53

19	K	Potassium	0.35	0.89	2.65	7.05	0.79	2.15	0.42	1.15
20	Ca	Calcium	0.2	0.5	0.54	1.46	0.79	2.2	1.26	3.57
22	Ti	Titanium	0	0	0	0	0	0	0.08	0.27
26	Fe	Iron	0.29	1.03	0	0	0.16	0.6	0.13	0.51

3.2 Optimization of Operating Conditions

3.2.1 Effect of Adsorbent Dosage

Adsorbent dosage study is an important parameter in adsorption studies, because it determines the capacity of adsorbent for a given initial concentration of metal solution. When the adsorbent dose was increased, the adsorption capacity (the amount adsorbed per unit mass of adsorbent) decreased using the adsorbent for the three metal ions.

The effect of adsorption of heavy metals on adsorbent dose was examined by varying the quantity of MHS from 0.1 to 0.7g per 50mL of the effluent while keeping the agitation rate at 250rpm and contact time of 30min. Fig 3.5 showed that as the adsorbent dose increased from 0.1 to 0.7g, the uptake capacity and percentage removal of Pb, As and Hg removed from the effluent significantly decreased. The percentage removal of Pb, As and Hg in this study, decreased with increasing adsorbent dosage. Increasing the dose from 0.1 to 0.7g led to a decrease in percentage removal of Pb, As and Hg from 58.7 to 35.2%, 69.8 to 18.7% and 100 to 34.6% on MHS respectively. The equilibrium adsorption capacity per unit mass of the adsorbents decreased considerably with increase in adsorbent dose for both metal ions. Increase in adsorbent dosage led to a decrease in the equilibrium adsorption capacity of Pb from 211.5 to 18.1 mg/g, As from 125 to 5.6 mg/g on MHS while that of Hg decreased from 13 to 0.6 mg/g on MHS. Optimum capacity and removal were achieved using 0.1g adsorbent dose with a maximum capacity of 211.5, 125 and 13 mg/g, and removal efficiency of 59%, 70%, and 100% for Pb, As, and Hg respectively. This result was subsequently used in all isotherms adsorption experiments.

The decrease in adsorption capacity with increase in the adsorbent dose was largely due to the increase of free adsorption sites. The decrease in the percentage adsorption of the three metal ions with increased adsorbent dose, could be due to denseness of the adsorbent particles at higher dosage (Batagarawa et al., 2017). This lead to decrease in the total surface area of the adsorbent particles available for the metal ions, thereby leading to decrease in amount of metal ions removed from the effluent.

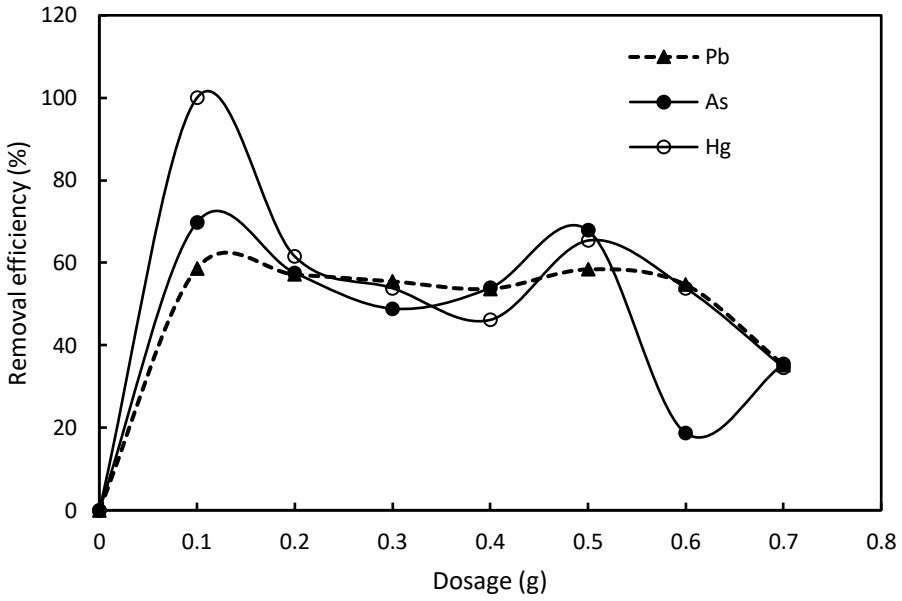

Figure 3.5: Effect of Adsorbent Dosage on heavy metals adsorption for MHS

3.2.2 Effect of Contact Time

Contact time is an important parameter that affects all transfer phenomena including adsorption process. The effect of contact time on the removal of Pb, As and Hg from industrial effluent was investigated at a contact time of 20, 40, 60, 80, 100 and 120 minutes and 250 rpm, using 0.1g adsorbent dose. It can be observed in Fig. 3.6 that, increase in the contact time from 20min to 120min increased the percentage removal for Pb, where 89.6% removal was achieved at 120min and this was chosen as the optimum time. The percentage removal of Hg from effluent using MHS has significantly decreased from 20min to 60min. However, increase in contact time from 60min to 80min led to significant increase in percentage removal from 30.8 to 65.4%. Thereafter the percentage removal of Hg decreased (from 65.4 to 53.8%) and ultimately increased (from 53.8 – 76.9%) due to increase in contact time from 80 to 100 min and 100 to 120 min respectively. The percentage of As removed using MHS increased as the contact time increased with highest percentage removal of 81.8% at 80min. However, the percentage removal for As decreased from 75.4 to 51.4% sequel to the increase in contact time from 20min to 40min. Further increase in contact time up to 60min had a positive effect on the amount removed.

With increased contact time, the rate of diffusion of metal ions from the effluent to the liquid boundary layer surrounding the adsorbent particles becomes high due to enhanced turbulence and decreased thickness of the liquid boundary layer (Sadiq, 2014). Rapid adsorption of metal ions

during the initial stage could be due to high concentration gradient between the adsorbate and the number of available vacant sites on the adsorbent surface (Gupta et al, 2004). Similar results were obtained by Bernard et al, (2013), where activated carbon prepared from coconut shell was used to remove Pb2+, Cu2+, Zn2+ and Fe2+ from industrial waste water.

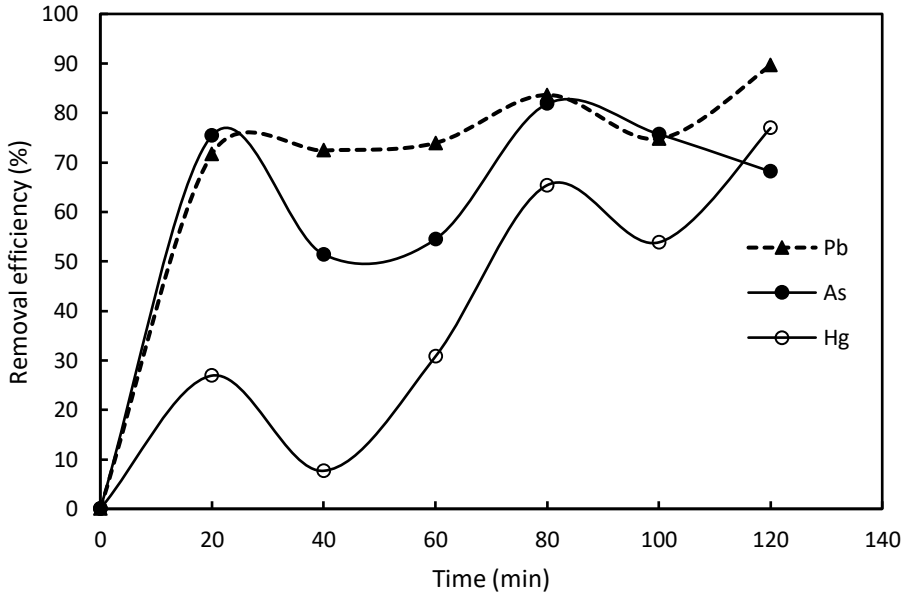

Figure 3.6: Effect of contact time on heavy metals adsorption for MHS

3.2.3 Effect of pH

pH plays significant role in controlling the adsorption of heavy metals. pH affects the activity of the functional groups on the adsorbent and the degree of ionization. Effect of pH on the adsorptive removal of Pb, As and Hg onto MHS, where chemical precipitation is almost avoided, so that metal removal could be related to the adsorption process. Figure 3.7 depicts the impact of the pH value of the effluent between 4.25 and 9.94 on the performance of the activated carbon at 50 mL of effluent, 0.1g adsorbent dosage and 30 min of contact time. The highest removal percentages of Pb, As and Hg was observed at pH 7.42 for MHS and there was a gradual decrease in the removal percentages as the pH moved from 4 to 9. The result shows that the removal efficiencies by MHS increased suddenly from 46.05 to 64.22% for Pb, 73.46 to 98.60% for As, and 11.53 to 69.23% Hg, with the pH increased from 4.25 to 7.42. However, when the pH was increased from 7.42 to 9.94, the removal efficiency of MHS was decreased to 66.02, 86.31 and 57.69% for Pb, As and Hg respectively. These may be attributed to the presence of a greater number of adsorbing sites on the adsorbent at lower pH which can absorb metal ions. The susceptibility of the system pH

changes may be attributed to the nature of the ions in solution and the nature of adsorbent used. The lower the pH, the more the H+ ions competing with the metal ions for adsorption sites, thus reduces their adsorption. On the other hand, the higher the pH the less the H+ ions competing with metal ions for adsorption sites, thus increasing their adsorption (Batagarawa & Ajibola, 2019).

At lower pH, the overall surface charge of the adsorbent will be positive and the adsorbent surface is surrounded by hydrogen ion (H+), this blocks the metal ions from binding sites of the adsorbents. As the solution pH increases, the adsorbent surface becomes deprotonated and more negatively charged surface becomes available hence an attraction between the positive metal cations occurs. The increase in metal ion adsorption with increase in pH was due to decrease in competition between hydrogen ion and metal ion for the surface site as a result of decrease in positive surface charge. At higher pH, precipitation of metal ions occurred, thus leading to decrease in adsorption of metal ions (Batagarawa et al., 2017). Similar trend was observed by Batagarawa & Ajibola, (2019) where Cr, Ni and Mn ions were removed from aqueous solution using Millet husk (Batagarawa et al., 2017).

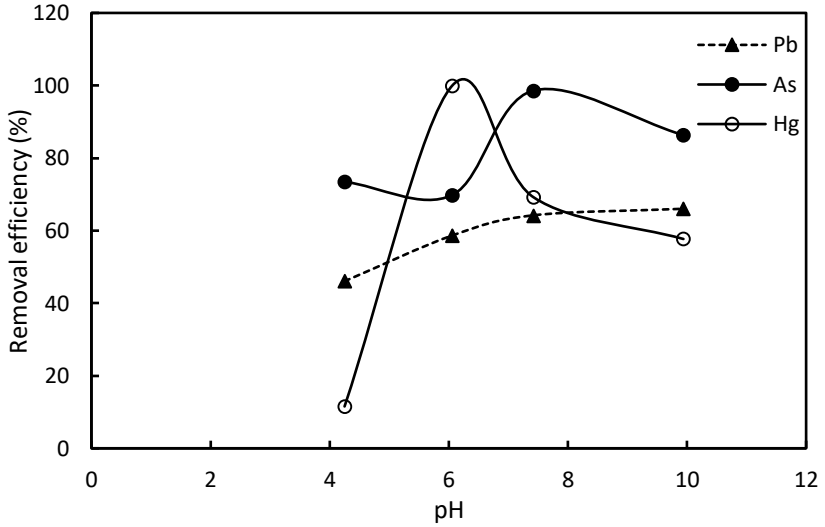

Figure 3.7: Effect of pH on heavy metals adsorption for MHS

3.2.4 Effect of Initial Concentration

The effect of Pb, As and Hg ions initial concentration was studied by varying the concentrations between 20–140 mg/l for Pb, As, and Hg using adsorbent dose (0.1 g), keeping pH at 7.42, agitation rate at 250 rpm, 25°C and 30 min contact time. The effect of varying concentrations on adsorption is shown in Figure 3.8(a-c) for Pb, As, and Hg. The adsorption responses of MHS were highly dependent on the initial concentrations in the solutions which are shown in Figure 3.8(a-c).

It can be seen from the results, by increasing the Pb, As and Hg ions initial concentration, the adsorption capacities increased, whereas percentage removal decreased as the initial concentration increased (Figure 3.8) The removal efficiency of MHS was highly dependent on the initial concentrations in the solutions. Highest percentage adsorption of Pb, As and Hg using MHS were 86.40%, 93.29% and 81.70% respectively. The increase in adsorption at the initial stage was due to the availability of vacant sites on the surface of the adsorbent. It is generally expected that as the concentration of the adsorbate increases the metal ions removed should increase. This result is in agreement with the expected trend. It is believed that increase in concentration of the adsorbate brings about increase in competition of adsorbate molecules for few available binding sites on the surface of the adsorbent, hence increasing the amount of metal ions removed (Batagarawa et al., 2017).

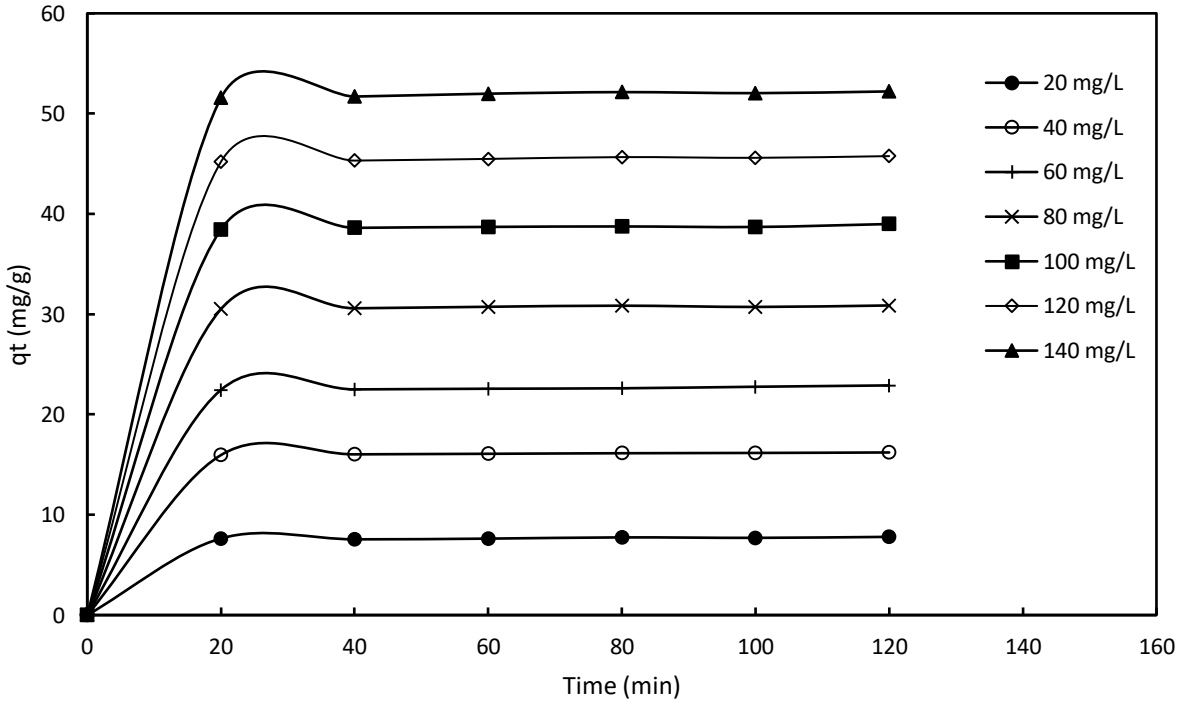

Figure 3.8a: Effect of Pb Initial Concentration on MHS

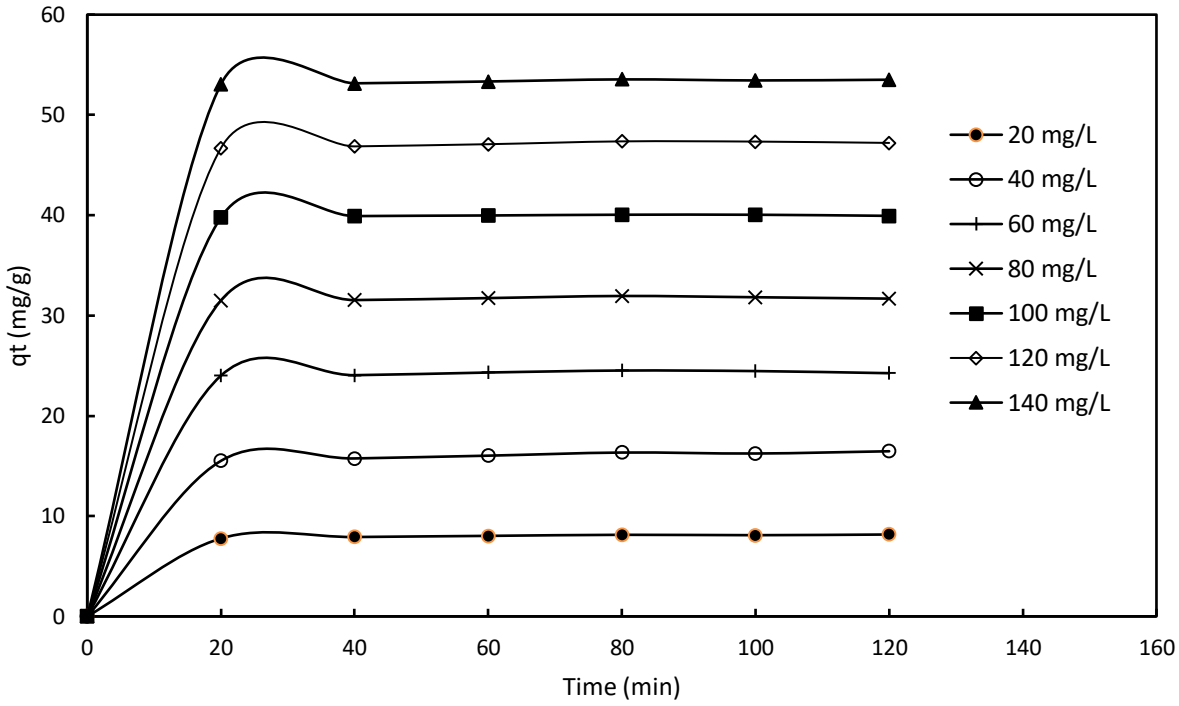

Figure 3.8b: Effect of As Initial Concentration on MHS

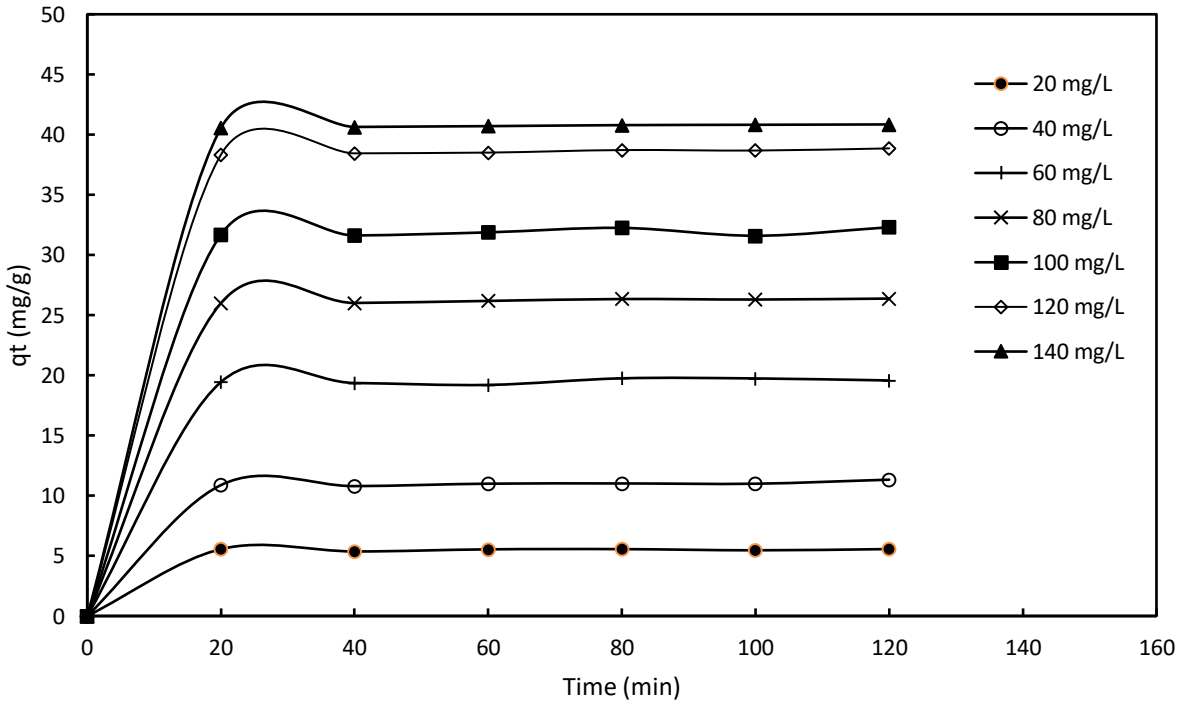

Figure 3.8c: Effect of Hg Initial Concentration on MHS

The study faced several limitations. Firstly, the agro-waste adsorbents have not been thoroughly characterized, lacking detailed analysis of surface area, and porosity, which are essential for understanding adsorption mechanisms. Additionally, the kinetics and equilibrium isotherms of adsorption have not been studied, limiting insights into the process. The use of real industrial effluents in adsorption studies offers more realistic insights but introduces limitations such as the complexity of contaminant mixtures, variability in effluent composition, potential interferences from suspended solids and organic matter, the need for pretreatment steps that increase costs, challenges in obtaining sufficient quantities for testing, and ethical and safety concerns related to hazardous substances, highlighting the importance of balancing these challenges with the benefits and considering a combination of synthetic and real effluent studies for robust wastewater treatment solutions. Moreover, the potential for regeneration and reuse of the adsorbents, impacting economic viability have not been explored. The study also was confined to laboratory-scale experiments without assessing pilot or field-scale applications. Finally, an evaluation of economic feasibility and environmental impacts related to the use of agro-waste adsorbents is lacking, which is vital for practical implementation.

4. Conclusion

Raw Millet husk and Raw Millet straw were used as precursors for the removal of Lead, Arsenic and Mercury from industrial effluents. The Raw Millet husk and Raw Millet straw were carbonized and subsequently activated with Sodium Hydroxide (NaOH) to obtained Millet Husk and Straw activated carbon (MHS). The MHS was characterized using Fourier Transform Infrared Spectroscopy (FTIR), X-ray diffraction (XRD), Scanning Electron Microscopy (SEM), and Energy dispersive x-ray spectroscopy (EDX). The Adsorption performance of the MHS on heavy metals (Lead, Arsenic and Mercury) was also carried out in a batch process. The industrial effluent sample was analyzed before and after Adsorption by Atomic Adsorption Spectrometry (AAS). The results showed that MHS adsorbent confirmed the presence of functional groups such as hydroxyl and alkanes with peaks at 3026.6, and 2922.2 cm-1 respectively, where the sharp peak at $2\theta=44.19°$ corresponds to crystalline peak associated with cellulosic carbon, and enhanced surface morphology with high porosity and better thermal stability, are present and played an important role in MHS adsorption. The effect of dosage on percentage removal of heavy metals revealed that as the dosage increases from 0.1-0.7g, the amount of metal ion adsorbed decreases, indicating

an optimal dosage for efficient removal, possibly due to particle aggregation, unsaturated adsorption sites, interference between sites, and increased solution viscosity, while the total removal may still increase, necessitating the determination of the optimal balance between percentage and total removal. The contact time was optimized for the maximum removal of heavy metals with the, adsorbent dosage 0.1g and pH 7.42 by varying the agitating time of (20-120 min). Lead, Arsenic and Mercury ions removal efficiency was found to be pH dependent. The As adsorption was higher at pH 7.42 (98.60%) and by increasing pH, the adsorption capacity decreases.

Authors contribution statement

Burah Tijjani developed the overall concept, gathered and analyzed the data, and wrote and revised the content. Ali Lawan Yaumi, Habiba D. Mohammed, Hamza Umar, Emmanuel Yakubu, and Bitrus Kwaji Highina provided valuable ideas, insights, and suggestions for improvement while also editing the content.

Conflict of interest statement

The authors declare no conflict of interest.

Acknowledgements

The authors acknowledge the cooperation of Hashimu Tijjani during the collection of the agro-wastes.

References

Abbas, A. F., & Ahmed, M. J., 2016. Journal of Water Process Engineering Mesoporous activated carbon from date stones (Phoenix dactylifera L .) by one-step microwave assisted K 2 CO 3 pyrolysis. *Journal of Water Process Engineering*, *9*, 201–207. https://doi.org/10.1016/j.jwpe.2016.01.004

Adegbola, R. Q., Otitodun, G. O. Okparavero, N. F., Jimoh, O. M., & Okunlade, A. F., 2023. Fact about Pearl Millet (Pennisetum Glaucum L .): A Review. *Iconic Research and Engineering Journals 6*(11), 605–615.

Ajikashile, J. O., Alhnidi, M., Bishir, M., & Kruse, A., 2023. The influence of torrefaction

temperature and reaction time on the properties of torrefied sun-dried millet and sorghum straws from the arid and semi-arid zones of western Africa. *Biofuels, Bioproducts and Biorefining* 751–767. https://doi.org/10.1002/bbb.2464

Al-ghouti, M. A., & Da'ana, D. A., 2020. Guidelines for the use and interpretation of adsorption isotherm models : A review. *Journal of Hazardous Materials*, *393*(November 2019), 122383. https://doi.org/10.1016/j.jhazmat.2020.122383

Alshameri, A., He, H., Zhu, J., Xi, Y., Zhu, R., Ma, L., & Tao, Q., 2017. Adsorption of ammonium by different natural clay minerals : Characterization , kinetics and adsorption isotherms. *Applied Clay Science*. https://doi.org/10.1016/j.clay.2017.11.007

Arslan, R. A., Pennells, J., Yamauchi, Y., Annamalai, P. K., Kumar, A., & Martin, D. J., 2022. Lignocellulosic plant cell wall variation influences the structure and properties of hard carbon derived from sorghum biomass. *Carbon Trends*, *7*, 100168. https://doi.org/10.1016/j.cartre.2022.100168

Batagarawa, S. M., & Ajibola, A. K., 2019. Comparative evaluation for the adsorption of toxic heavy metals on to millet , corn and rice husks as adsorbents. *Journal of Analytical & Pharmaceutical Research Research,* *8*(3), 119–125. https://doi.org/10.15406/japlr.2019.08.00325

Batagarawa, S. M., & Dayo, L. Y., 2017. Millet husk as efficient adsorbent for removal of lead, cadmium, and nickel ions from aqueous solution. *Dutse Journal of Pure and Applied Sciences (DUJOPAS), 3*(1).

Bedmohata, M. A., Chaudhari, A. R., Singh, S. P., & Choudhary, M. D., 2015. Adsorption Capacity of Activated Carbon Prepared by Chemical Activation of Lignin for the Removal of Methylene Blue Dye. *International Journal of Advanced Research in Chemical Science (IJARCS), 2(8),* 1-13.

Büyükgüngor, H., & Orhan, Y., 2018. The removal of heavy metals by using agricultural wastes. *Wat. Sci. Tech.*, 28(2), 247-155.

Byamba-ochir, N., Shim, W. G., Balathanigaimani, M. S., & Moona, H., 2016. Highly Porous Activated Carbons Prepared from Carbon Rich Mongolian Anthracite by Direct NaOH Activation. *Applied Surface Science*. https://doi.org/10.1016/j.apsusc.2016.04.082

Elavasaran, A., 2018. EDX and XRD, FT-IR Spectra, Analysis Containing Hexavalent Chromium Metal ion Adsorption Present in Aqueous Solution onto Phosphoric Acid (H_3PO_4) Activated

Mimusops Elengi Leaves Carbon. *Journal of Drug Delivery and Therapeutics, 8(5-s),* 132-138. https://dx.doi.org/10.22270/jddt.v8i5-s.1917

Hammajam, A. A., Ismarrubie. N. Z., Salit, M. S., & Zulkiffle, L., 2017. Characterization of Millet (Pennisetum glaucum) Husk Fiber (MHF) and Its Use as Filler for High Density Polyethylene (HDPE) Composites. *BioResources 12*(4), 9287-9301.

Hashem, A., Al-anwar, A., Nagy, N. M., Hussein, D. M., & Eisa, S., 2016. Isotherms and kinetic studies on adsorption of Hg (II) ions onto Ziziphus spina-christi L . from aqueous solutions. *Green Process Synth, 5*, 213–224. https://doi.org/10.1515/gps-2015-0103

Ignatowicz, K., 2017. The impact of sewage sludge treatment on the content of selected heavy metals and their fractions. *Environmental Research*, *156*, 19–22. https://doi.org/10.1016/j.envres.2017.02.035

Joga Rao, H., 2021. Characterization Studies on Adsorption of Lead and Cadmium Using Activated Carbon Prepared from Waste Tyres. *Nature Environment and Pollution Technology, 20(2),* 561-568. https://doi.org/10.46488/NEPT.2021.v20i02.012

Khan, R., Saxena, A., Shukla, S., Sekar, S., Senapathi, V., & Wu, J., 2021. Environmental contamination by heavy metals and associated human health risk assessment : a case study of surface water in Gomti River Basin , India. *Environmental Science and Pollution Research, 126*. https://doi.org/10.1007/s11356-021-14592-0

Nallakukkala, S., Rehman, A., Zaini, D. B., & Lal, B., 2022. Gas Hydrate-Based Heavy Metal Ion Removal from Industrial. *Water, 14,* 1171. https://doi.org/10.3390/w14071171

Omeje, K. O., Ezema, B. O., Okonkwo, F., Onyishi, N. C., Ozioko, J., Rasaq, W. A., Sardo, G., & Okpala, C. O. R., 2021. Quantification of Heavy Metals and Pesticide Residues in Widely Consumed Nigerian Food Crops Using Atomic Absorption Spectroscopy (AAS) and Gas Chromatography (GC). *Toxins, 13,* 870. https://doi.org/ 10.3390/toxins13120870

Prajapati, A. K., Verma, P., Singh, S., & Mondal, M. K., 2022. Adsorption-Desorption Surface Bindings , Kinetics , and Mass Transfer Behavior of Thermally and Chemically Treated Great Millet Husk towards Cr (VI) Removal from Synthetic Wastewater. *Adsorption Science & Technology, 2022*(Vi). https://doi.org/10.1155/2022/3956977

Qasem, N. A. A., Mohammed, R. H., & Lawal, D. U., 2021. Removal of heavy metal ions from wastewater : a comprehensive and critical review. *Nature Partner Journals*. https://doi.org/10.1038/s41545-021-00127-0

Samsuri, A. W., Sadegh-Zadeh, F., & Seh-Bardan, B. J., 2013. Characterization of biochars produced from oil palm and rice husks and their adsorption capacities for heavy metals. *Int. J. Environ. Sci. Technol.,* Vi. https://doi.org/10.1007/s13762-013-0291-3

Siswati, S., Pratama, H., & Giatman, M., 2023. Adsorption Using Fly Ash from Stam Power Plants for Acid Mine Drainage Treatment. IOP Conference Series: *Earth and Environmental Science. 1173(2023)* 012040. https://doi.org10.1088/1755-1315/1173/1/012040

Tatah, V.S., Otitoju, O., Ezeonu, C. S., Onwurah I. N. E., & Ibrahim K. L. C., 2017. Characterization and Adsorption Isotherm Studies of Cd (II) And Pb (II) Ions Bioremediation from Aqueous Solution Using Unmodified Sorghum Husk. *Journal of Applied Biotechnology & Bioengineering, 2*(3). https://doi.org/10.15406/jabb.2017.02.00034

Wang, H., & Matsushita, M. T., 2021. Heavy metals and adult neurogenesis. *Current Opinion in Toxicology*, *26*, 14–21. https://doi.org/10.1016/j.cotox.2021.03.006

Yadav, M., Rengasamy, R. S., & Gupta, D., 2019. Characterization of Pearl Millet (Pennisetum glaucum) waste. *Carbohydrate Polymers*, *212*(February), 160–168. https://doi.org/10.1016/j.carbpol.2019.02.034

Yakout, S. M., & El-deen, G. S., 2016. Characterization of activated carbon prepared by phosphoric acid activation of olive stones. *Arabian Journal of Chemistry*, *9*, S1155–S1162. https://doi.org/10.1016/j.arabjc.2011.12.002